ICONTECH INTERNATIONAL JOURNAL OF SURVEYS, ENGINEERING, TECHNOLOGY
ISSN 2717-7270
Journal homepage: http://icontechjournal.com/index.php/iij
Volume 7 (2023) Issue 2

COMPUTATIONAL ANALYSIS OF FLOW CHARACTERISTICS OF NOZZLES WITH DIFFERENT GEOMETRIES

Mert Son

Mersin University, Vocational School of Technical Sciences, 33343, Yenişehir, Mersin, Türkiye.

ORCID ID: 0000-0003-4553-1991

Bünyamin Demir

Mersin University, Department of Mechanical Engineering, 33340, Mersin, Türkiye.

ORCID ID: 0000-0002-6405-4724

Abstract

In this study, five different nozzles which can be used for spraying operations were generated and flow analyses of these nozzles were carried with the use of Computational Fluid Dynamics and Finite volume analysis software. Flow analyses were carried out for each nozzle geometry and the effect of the nozzle geometry on the velocity of fluid was investigated. It was determined that nozzle geometry influenced the velocity of the fluid. During the analysis processes, three different turbulence models (k-omega, k-epsilon and transition k-kl omega) were selected to investigate the effect of turbulence model on velocity of the fluid. Present analyses revealed that these turbulence model did not have any remarkable effects on the velocity of the fluid but influenced spray distribution area.

Keywords: Nozzle, CFD, turbulence, Spraying

1. Introduction

Spraying applications, which are widely used in many sectors such as textile, dyeing, cleaning, agriculture, food, automotive, air conditioning, food coating, fuel injection in internal combustion engines, pesticides and irrigation, personal care in daily life applications, cosmetics etc.

Spraying is the process of transferring the fluid to the target surface in the form of small droplets and particles by giving high velocity and pressure to the fluid, instead of directly transferring any fluid to another surface or target area. The reason why this process is preferred in many industrial areas is to prevent the use of excess fluid by giving the fluid to be transferred to the environment in droplet form and to use the fluid to be used with the highest efficiency without wasting it. In order to the spraying process to take place, the fluid to be transferred must have a certain velocity and pressure value, mechanical parts are used that bring the fluid to this velocity and pressure after leaving its source and turn the kinetic energy of the fluid into small particles. These mechanical parts are called nozzles [1].

There are many different types of nozzles used in the industrial field, nozzles are usually named according to the type of fluid they transfer or the boundary areas they affect on the surface in the spraying process. Some commonly used nozzles are hydraulic nozzles, pneumatic nozzles, air nozzles, fan nozzles, empty conical nozzles, filled conical nozzles,

Received 25 May 2023; Received in revised form 10 June 2023; Accepted 20 June 2023;
Available online 30 June 2023;
doi: 10.5281/zenodo.8130808

point spray nozzles and fog nozzles. Nozzles, which are frequently used in industrial areas and appear in a wide variety of structures, have a very relevant role in the quality of the final product and spray efficiency in the systems they will be used, so it is very important to choose the nozzle to be used in spraying operations in accordance with the system to which it will be integrated and the desired post-processing requirements [1]. Onen et al. emphasized in a study that one of the most influential factors affecting the abrasive particle velocity and the damage mechanism in the target material in erosive wear is the geometry of the nozzle. Researchers have reported that different nozzle geometries can be used in many different applications such as micro-abrasive jet machining and sandblasting. In addition, researchers stated that abrasive blasting applications are one of the traditional abrasive material processing methods and have many uses such as micro-abrasive jet processing, surface treatment, surface cleaning [2]. In order to see the effects of nozzle selection, instead of using experimental systems, the system in which the nozzle will operate can be simulated and flow analyzes can be made using a finite element method program with computational fluid dynamics methods, so that necessary analyzes can be made before the nozzle is used and the suitability of the nozzle can be determined before use.

Meyer and Lupoi investigated the nozzles with three different designs used in cold spraying applications under standard operating conditions, and carried out the coating efficiency and particle flow analysis with the computational fluid dynamics methods on nozzles with three different designs. As a result of the research; when titanium was chosen as the coating material, it was determined that there was a direct corresponding relationship between the coating efficiency and the nozzle cross-sectional area. As a result of the experiments, it was observed that the coating efficiency of the nozzle with the smallest cross-sectional area was also the lowest [3].

Yin et al. investigated the effects of nozzle cross-sectional area on gas flow and particle acceleration in spraying operations. In the study, they compared a rectangular nozzle with an elliptical nozzle model, and as a result of the study, it was determined that the particle velocity was higher in the elliptical geometry nozzle than in the rectangular geometry nozzle [4]. Zeng et al. reported that nozzle geometry, accelerated gas and particle properties directly affect the particle impact rate [5].

In this study, nozzle geometries with five different interior designs that can be used in spraying operations were created and a water flow analysis was performed in ANSYS fluent software. On the basis of the analysis, the changes in the outlet velocity and pressure due to different geometries of the fluid with the same inlet velocity and pressure were examined.

2. Materials and Methods

In this study, five different nozzle geometries were created using the Design Modeler application of the ANSYS Workbench software. During the nozzle design, the nozzle inlet and outlet diameters were designed to be the same, and only dimensional changes were made in the inner geometry of the nozzle. After the design step, water flow analysis was performed for five different nozzles and flow analysis was performed using three different turbulence models.

Received 25 May 2023; Received in revised form 10 June 2023; Accepted 20 June 2023;
Available online 30 June 2023;
doi: 10.5281/zenodo.8130808

For the flow analysis, water was used as the fluid and the fluid inlet velocity was determined as 5 m/s and the fluid inlet pressure was determined as 1 bar. Analyzes were made by applying three different turbulence models for each design.

2.1. Computational Fluid Dynamics

Fluid dynamics is the science that studies fluid motion. There are three basic approaches in fluid dynamics, these are; experimental, numerical and theoretical approaches. In computational fluid dynamics, the fluid is modeled as a continuum and this method is a computer-based engineering method. Computational fluid dynamics is a method that is generally used to examine and analyze systems that are impossible to study experimentally [6,7].

2.2. Finite Element Method

The finite element method is one of the important numerical methods widely used in solving many problems in the fields of physics and engineering. The basis of the finite element method

is based on the principle of modeling complex structures with smaller structures that can perform calculations. In this method, the structure to be analyzed is handled in small parts and the analyzes are made on these small structures and the results are reported [8].

2.3. Finite Volume Method

The Finite Volume Method is a numerical technique that leverages conservation laws in order to convert partial differential equations into solvable algebraic equations. It is widely used in the fields of fluid mechanics, heat transfer. Ansys fluent software solves partial differential equations problems based on finite volume method [9].

2.4. Basic Differential Equations of Fluid Mechanics

It is quite difficult and complex to analyze the differential equations of fluid motion; what is known about their general mathematical properties is quite insufficient. On the other hand, some things of great educational value are viable. It reveals the basic dimensionless parameters that organize the motion of the fluid, even if the equations are not solved at first. Considerable amount of useful solutions can be obtained if steady flow and incompressible flow assumptions are made. A third and rather major simplification is the assumption of frictionless flow. This acceptance validates the Bernoulli equation, providing a wide variety of idealized, or ideal fluid, possible solutions [10].

2.4.1. Continuity and Navier-Strokes Equations

The Navier-Stokes and continuity equations are the most common flow equations that can be used in flow analysis. The continuity equation expresses the mass conservation law of the fluid passing through a control volume in differential dimensions, while the Navier-Stokes

Received 25 May 2023; Received in revised form 10 June 2023; Accepted 20 June 2023;
Available online 30 June 2023;
doi: 10.5281/zenodo.8130808

equations express the conservation of motion equations formed by the application of Newton's second law to the control volume. Continuity and motion equations for a Newtonian and incompressible flow with constant physical properties in Cartesian coordinates are written as follows [11].

$$\frac{\partial \rho}{\partial t}+\frac{\partial(\rho u)}{\partial x}+\frac{\partial(\rho v)}{\partial y}+\frac{\partial(\rho w)}{\partial z}=0 \tag{1}$$

$$\rho\left(\frac{\partial u}{\partial t}+u\frac{\partial u}{\partial x}+v\frac{\partial u}{\partial y}+w\frac{\partial u}{\partial z}\right)=-\frac{\partial p}{\partial x}+\mu\left(\frac{\partial^2 u}{\partial x^2}+\frac{\partial^2 u}{\partial y^2}+\frac{\partial^2 u}{\partial z^2}\right) \tag{2}$$

$$\rho\left(\frac{\partial v}{\partial t}+u\frac{\partial v}{\partial x}+v\frac{\partial v}{\partial y}+w\frac{\partial v}{\partial z}\right)=-\frac{\partial p}{\partial y}+\mu\left(\frac{\partial^2 v}{\partial x^2}+\frac{\partial^2 v}{\partial y^2}+\frac{\partial^2 v}{\partial z^2}\right) \tag{3}$$

(3)

$$\rho\left(\frac{\partial w}{\partial t}+u\frac{\partial w}{\partial x}+v\frac{\partial w}{\partial y}+w\frac{\partial w}{\partial z}\right)=-\frac{\partial p}{\partial z}+\mu\left(\frac{\partial^2 w}{\partial x^2}+\frac{\partial^2 w}{\partial y^2}+\frac{\partial^2 w}{\partial z^2}\right) \tag{4}$$

2.5. Turbulence Models

Turbulent flow is a problem that cannot be fully resolved and often cannot be solved in a meaningful way in classical physics. The turbulence of many problems in engineering has led to the development of models known as "turbulence models". Models are systematic mathematical derivations based on Navier-Stokes equations up to a certain point, as well as hypotheses based on dimensional argument and empirical inputs [7].

2.5.1. Two Equation Turbulence Models

It is extensively used in two-equation turbulence models because it has a good balance between numerical effort and computational accuracy. Two-equation models are much more complex than zero-equation models. Velocity and length scales are solved independently using the transport equations. For this reason, it is called a two-equation model. The k-ε and k-ω two-equation models use mean velocity gradients and gradient diffusion hypotheses due to turbulent viscosity Reynolds stresses. Turbulent viscosity is modeled according to velocity and turbulence length scales [12].

2.5.1.1. Standart k-ε Model

In the standard k-ε model, the convection equations of turbulent kinetic energy (k) and sloshing loss rate (ε) are solved and the turbulent momentum diffusion coefficient (viscosity) is calculated as a function of k and ε values [13].

Received 25 May 2023; Received in revised form 10 June 2023; Accepted 20 June 2023;
Available online 30 June 2023;
doi: 10.5281/zenodo.8130808

$$\frac{\partial}{\partial t}(\rho k)+\frac{\partial}{\partial x_i}(\rho k u_i)=\frac{\partial}{\partial x_j}\left[\left(\mu+\frac{\mu_t}{\sigma_k}\right)\frac{\partial k}{\partial x_j}\right]+G_k+G_b-\rho\varepsilon-Y_M+S_k \tag{5}$$

$$\frac{\partial}{\partial t}(\rho\varepsilon)+\frac{\partial}{\partial x_i}(\rho\varepsilon u_i)=\frac{\partial}{\partial x_j}\left[\left(\mu+\frac{\mu_t}{\sigma_\varepsilon}\right)\frac{\partial \varepsilon}{\partial x_j}\right]+C_{1\varepsilon}\frac{\varepsilon}{k}(G_k+C_{3\varepsilon}G_b)-C_{2\varepsilon}\rho\frac{\varepsilon^2}{k}+S_\varepsilon \tag{6}$$

2.5.1.2. Standart k-ω Model

This method developed by Wilcox [13]; It has updates for lower Re numbers, compressibility, and stress-induced flows. It is a disadvantage that it has sensitivity on the slip layer. The convection equations for turbulent kinetic energy (k) and attenuation rate (ω) prevailing in the model are given below.

$$\frac{\partial}{\partial t}(\rho k)+\frac{\partial}{\partial x_i}(\rho k u_i)=\frac{\partial}{\partial x_j}\left(\Gamma_k\frac{\partial k}{\partial x_j}\right)+G_k-Y_k \tag{7}$$

$$\frac{\partial}{\partial t}(\rho \omega)+\frac{\partial}{\partial x_i}(\rho \omega u_i)=\frac{\partial}{\partial x_j}\left(\Gamma_\omega\frac{\partial \omega}{\partial x_j}\right)+G_\omega-Y_\omega \tag{8}$$

In both equations, G terms represent the generation of turbulent kinetic energy, Y terms represent the rate of subduction, w S and k S represent sources. The effective diffusion symbols are expressed as Γk and Γω. All these terms are modeled. For flows with low Re coefficients, the correction and diffusion coefficients are embedded in swash viscosity terms. Compressibility correction is included in the model but not recommended for use in all general applications[12].

2.5.2. Three Equations Turbulence Models

2.5.2.1. Transistion k-kl Omega Model

Transition k-kl omega equation is a 3-equation turbulence model used mostly in transitional flows in flow analysis. This model is the model that can most accurately analyze the characteristics of the transitional flow in the boundary layer.

Received 25 May 2023; Received in revised form 10 June 2023; Accepted 20 June 2023;
Available online 30 June 2023;
doi: 10.5281/zenodo.8130808

$$\frac{Dk_T}{D} = P_{K_T} + R + R_{NAT} - \omega k_T - D_T \frac{\partial}{\partial x_j}\left[\left(v + \frac{\alpha_T}{\alpha_k}\right)\frac{\partial k_T}{\partial x_j}\right] \tag{9}$$

$$\frac{Dk_L}{D_t} = Pk_L - R - R_{NAT} D_L + \frac{\partial}{\partial x_j}\left[v \frac{\partial k_L}{\partial x_j}\right] \tag{10}$$

$$\frac{D_\omega}{D_t} = C_{\omega 1}\frac{\omega}{k_T} P_{K_T} + \left(\frac{C_{\omega R}}{f_W} - 1\right)\frac{\omega}{k_T}(R + R_{NAT}) - C\omega_2 \omega^2 + C\omega_3 f_\omega \alpha_T f_W^2 \frac{\sqrt{k_T}}{d^3} + \frac{\partial}{\partial x_j}\left[\left(v + \frac{\alpha_\gamma}{\alpha_\omega}\right)\frac{\partial \omega}{\partial x_j}\right] \tag{11}$$

By using the ANSYS Fluent software, the theoretical equations used in the fluid mechanics applications mentioned above are analyzed and flow analysis results are obtained. The figures below show five different nozzle designs and dimensions.

2.6. Nozzle Geometries

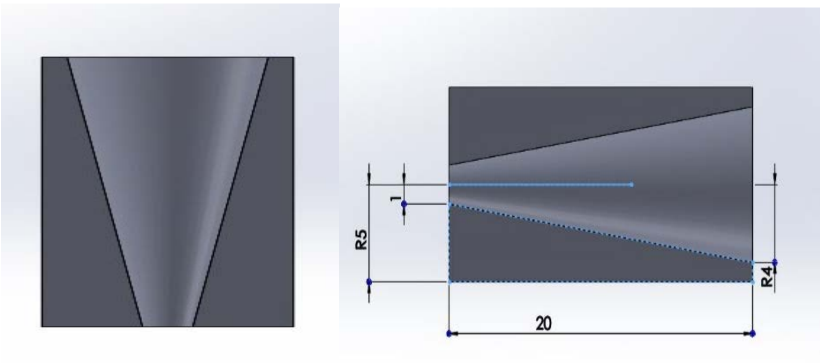

Figure 1. Design and Dimensions of First Nozzle.

Figure 2. Design and Dimensions of Second Nozzle.

Received 25 May 2023; Received in revised form 10 June 2023; Accepted 20 June 2023;
Available online 30 June 2023;
doi: 10.5281/zenodo.8130808

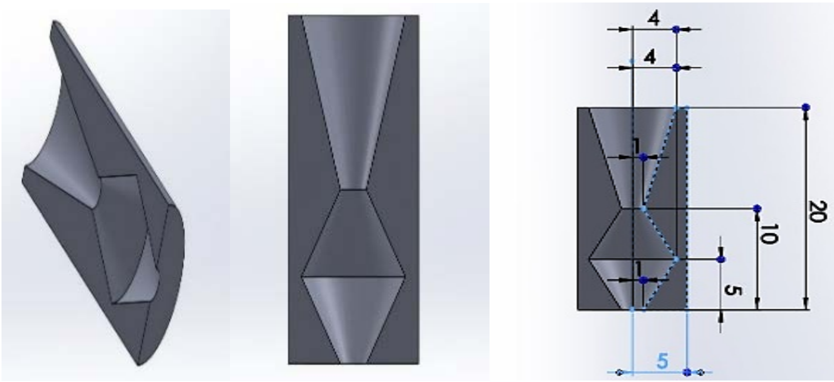

Figure 3. Design and Dimensions of Third Nozzle.

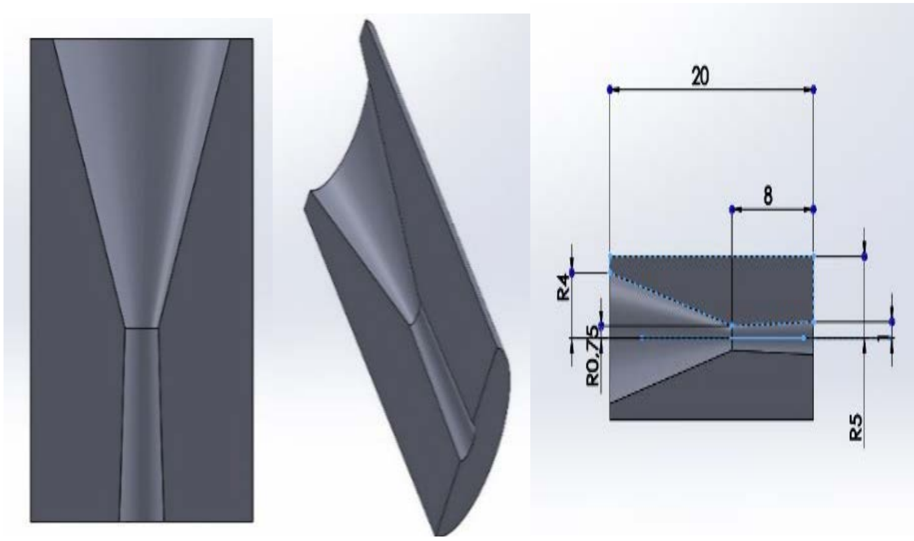

Figure 4. Design and Dimensions of Fourth Nozzle.

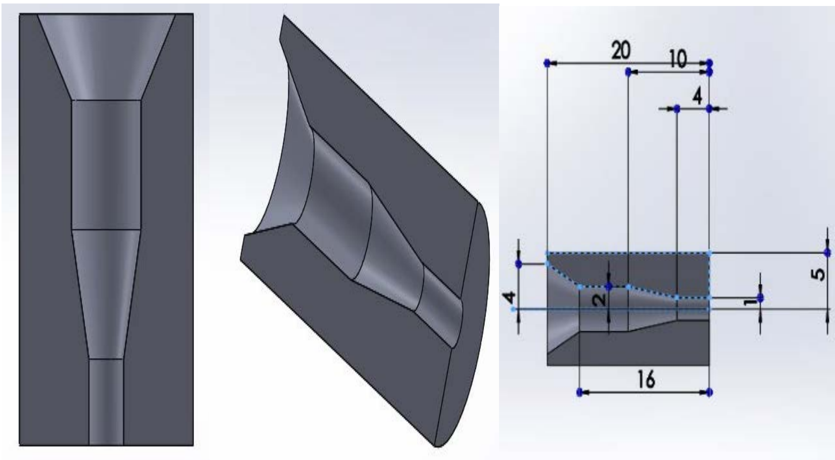

Figure 5. Design and Dimensions of Fifth Nozzle.

Received 25 May 2023; Received in revised form 10 June 2023; Accepted 20 June 2023;
Available online 30 June 2023;
doi: 10.5281/zenodo.8130808

The designs were first drawn in the SOLIDWORKS program. In order to perform the flow analysis in the ANSYS program, the drawings were made in two dimensions using the Design Modeler module of the ANSYS program using the same dimensions, and in the next step, a three-dimensional solid model was created. After the solid model was created, a control volume area was created to determine in which area the analysis would take place. After the control volume area was created, the meshing process was completed.

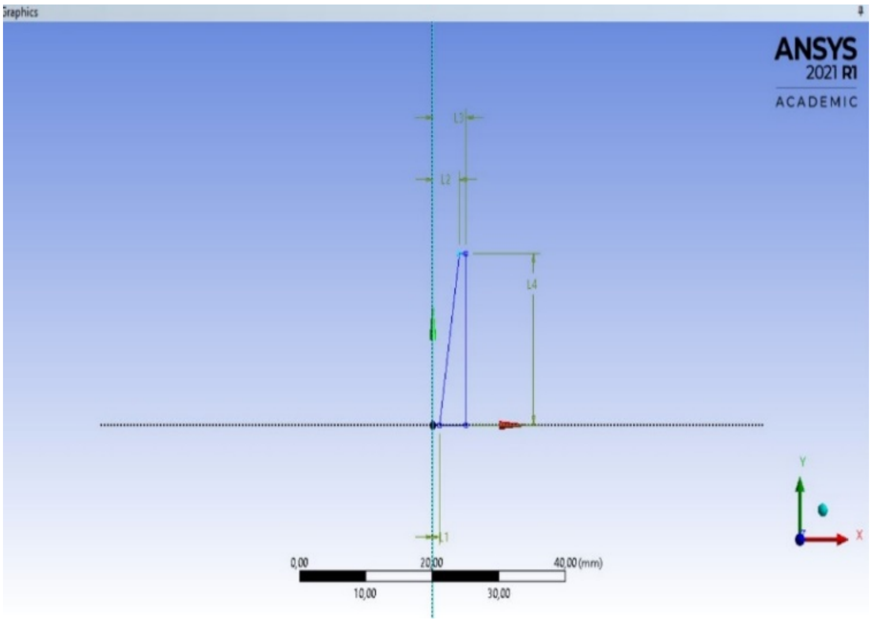

Figure 6. Two Dimension Drawing in the Design Modeler Section.

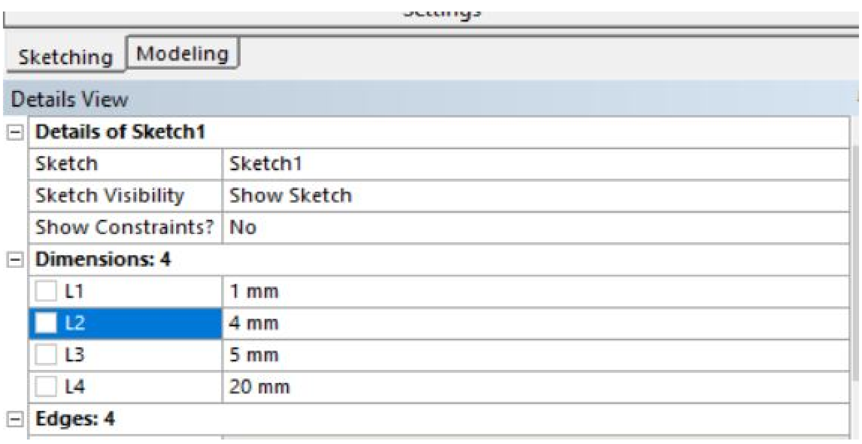

Sketching | Modeling

Details View

Details of Sketch1	
Sketch	Sketch1
Sketch Visibility	Show Sketch
Show Constraints?	No
Dimensions: 4	
L1	1 mm
L2	4 mm
L3	5 mm
L4	20 mm
Edges: 4	

Figure 7. Dimensioning View of the Modelling.

After the meshing process was completed, the nozzle inlet, outlet and body regions were assigned. After this process, the turbulence model was selected and the results were obtained after the analysis was performed according to these models.

Received 25 May 2023; Received in revised form 10 June 2023; Accepted 20 June 2023;
Available online 30 June 2023;
doi: 10.5281/zenodo.8130808

ICONTECH INTERNATIONAL JOURNAL OF SURVEYS, ENGINEERING, TECHNOLOGY
ISSN 2717-7270
Journal homepage: http://icontechjournal.com/index.php/iij
Volume 7 (2023) Issue 2

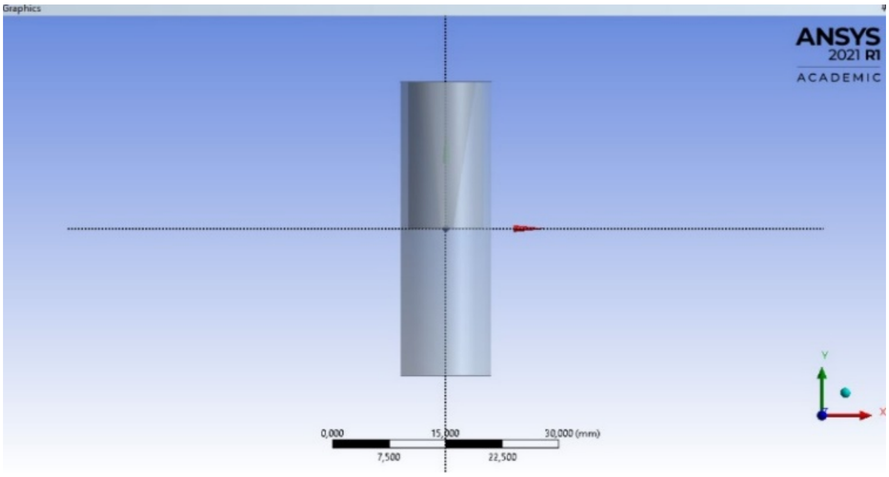

Figure 8. Determination of Control Volume Area.

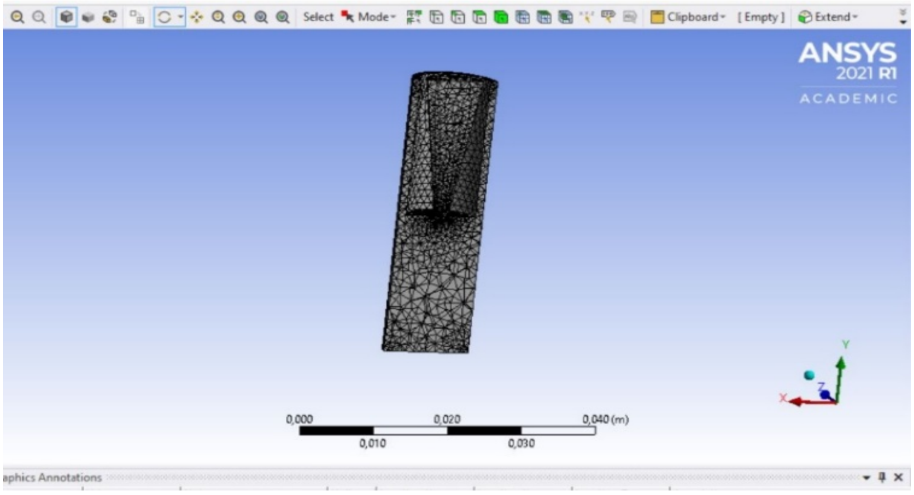

Figure 9. Meshing Process.

Received 25 May 2023; Received in revised form 10 June 2023; Accepted 20 June 2023;
Available online 30 June 2023;
doi: 10.5281/zenodo.8130808

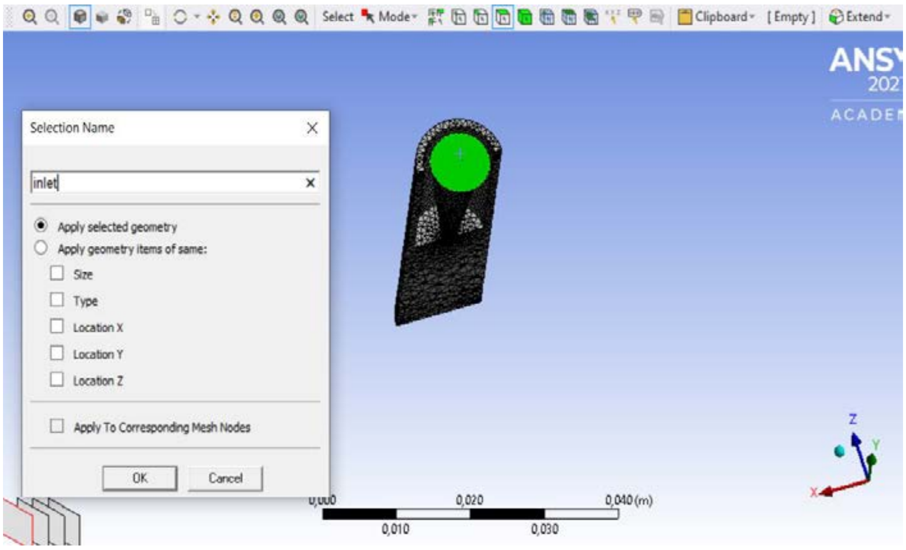

Figure 10. Defining the Inlet Zone of the Nozzle.

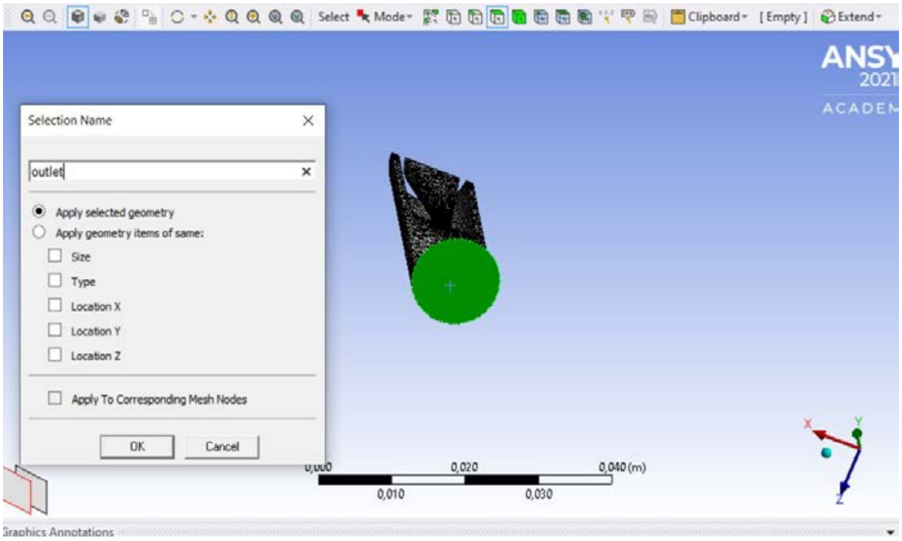

Figure 11. Defining the Outlet Zone of the Nozzle.

Received 25 May 2023; Received in revised form 10 June 2023; Accepted 20 June 2023;
Available online 30 June 2023;
doi: 10.5281/zenodo.8130808

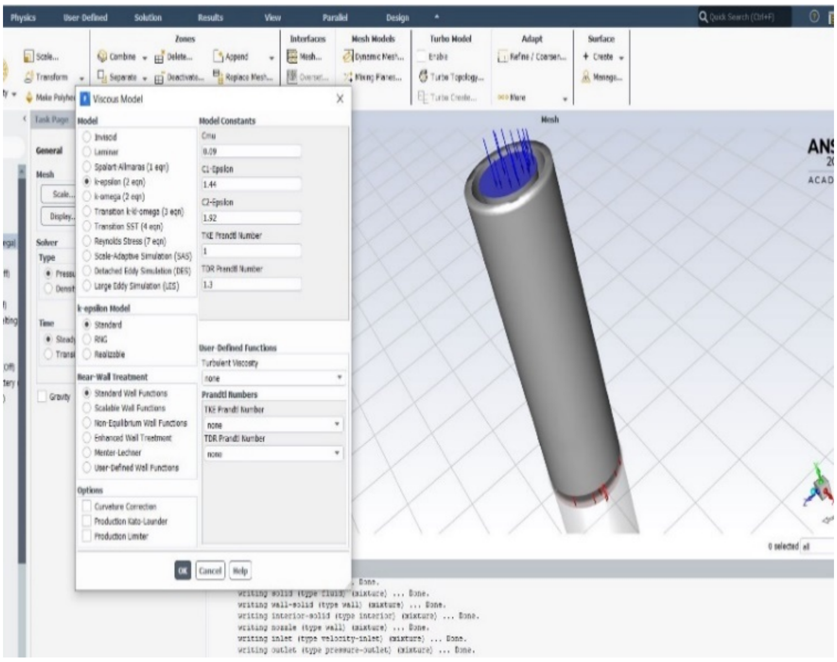

Figure 12. Determination of Turbulence Model.

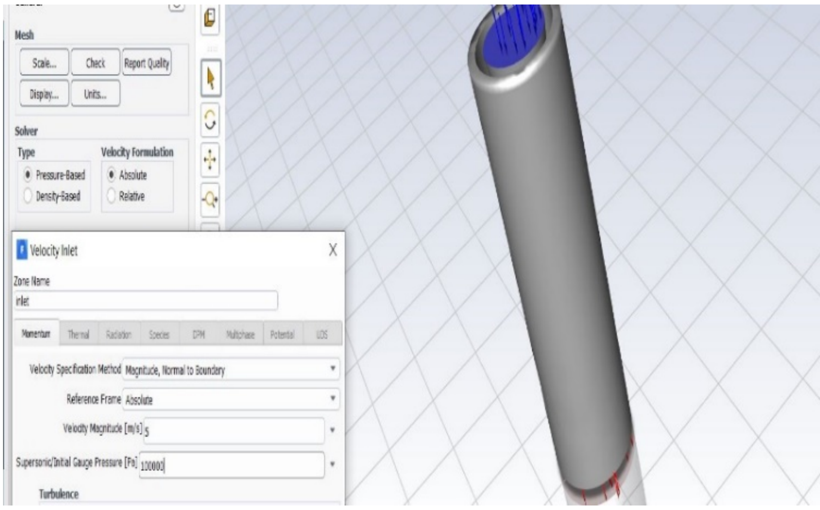

Figure 13. Determination of Boundary Conditions.

3. Results and Discussion

As a result of the analyzes made using 5 different nozzle materials in the research, the velocity values found on the basis of k-epsilon, k-omega and transition k-kl omega models are given in Table 1. In the results of the research, flow velocity distribution pictures of the analyzes performed with the K-Epsilon turbulence model, which is widely used in flow analysis, are given, and the results of the analysis made with other turbulence models are shown in the table. According to our research findings, it was determined that nozzle geometry significantly affects fluid velocity at nozzle outlet. However, it was determined that the change in turbulence patterns did not have a great effect on the spray rates of the nozzles

Received 25 May 2023; Received in revised form 10 June 2023; Accepted 20 June 2023;
Available online 30 June 2023;
doi: 10.5281/zenodo.8130808

(Table 1). The research results of Shipway and Hutchings [14] and Onen [15] who work on nozzle geometries, support our finding

Table 1. Comparison of Outlet Velocity Values of Fluids

	Fluid Velocities According to Turbulence Models		
Nozzles	Standart k-ε Model	K-Omega Standart k-ω Model	Transition k-kl Omega
1. Nozzle	88.41 m/s	87.48 m/s	88.24 m/s
2. Nozzle	94.81 m/s	94.41 m/s	93.81m/s
3. Nozzle	102.7 m/s	99.87 m/s	99.97 m/s
4. Nozzle	138.30 m/s	137.50 m/s	139.7 m/s
5. Nozzle	84.49 m/s	82.91 m/s	88.67 m/s

When the k-epsilon model was chosen as the turbulence model in the flow analysis with the first nozzle geometry, it was found that the velocity of the fluid reached 88.41 m/s at the outlet of the nozzle (Figure 14)

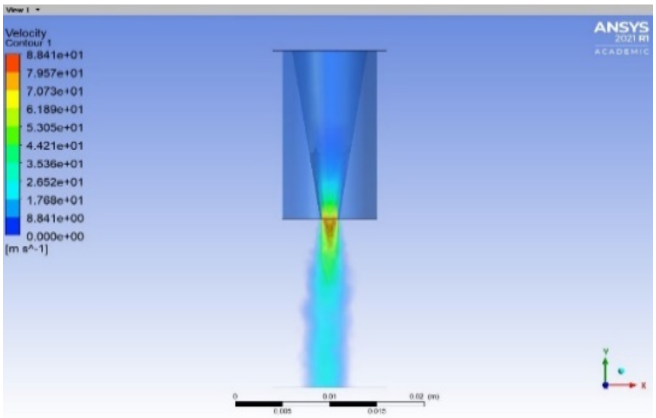

Figure 14. First Nozzle fluid Velocity Distribution (K-epsilon model).

According to the flow analysis made with the second nozzle geometry, when the k-epsilon model was chosen as the turbulence model, it was determined that the velocity of the fluid at the nozzle outlet reached 94.87 m/s at the nozzle outlet (Figure 15).

Received 25 May 2023; Received in revised form 10 June 2023; Accepted 20 June 2023;
Available online 30 June 2023;
doi: 10.5281/zenodo.8130808

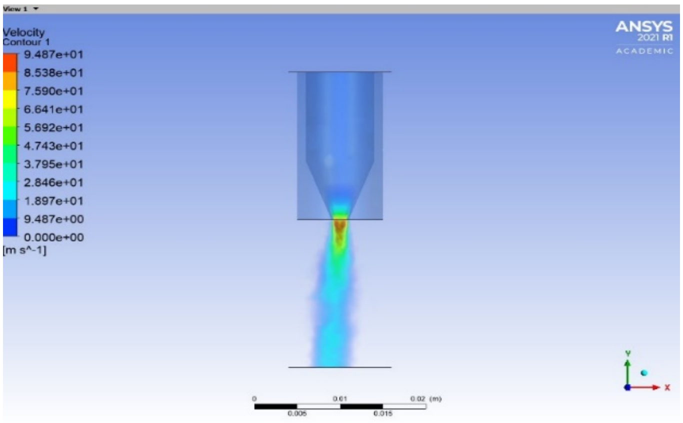

Figure 15. Second Nozzle Fluid Velocity Distribution (K-epsilon Model).

In the flow analysis made with the third nozzle geometry, when the k-epsilon model was used as the turbulence model, it was determined that velocity of the fluid reached to 102.7 m/s from 5 m/s at the nozzle exit. As can be seen in Figure 16, an increase in velocity was observed in the part of the nozzle geometry where the diameter narrowing occurred.

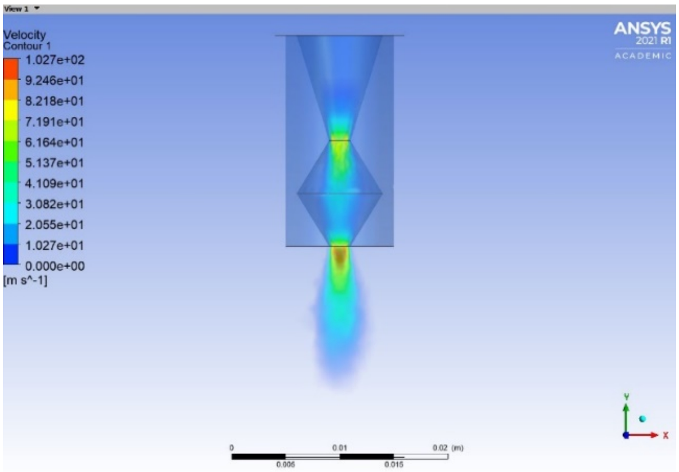

Figure 16. Third Nozzle Fluid Velocity Distribution (K-epsilon Model).

In the flow analysis made with the fourth nozzle geometry, when the k-epsilon model was chosen as the turbulence model, it was determined that velocity of the fluid reached a velocity of 138.30 m/s at the nozzle outlet (Figure 17).

Received 25 May 2023; Received in revised form 10 June 2023; Accepted 20 June 2023;
Available online 30 June 2023;
doi: 10.5281/zenodo.8130808

ICONTECH INTERNATIONAL JOURNAL OF SURVEYS, ENGINEERING, TECHNOLOGY
ISSN 2717-7270
Journal homepage: http://icontechjournal.com/index.php/iij
Volume 7 (2023) Issue 2

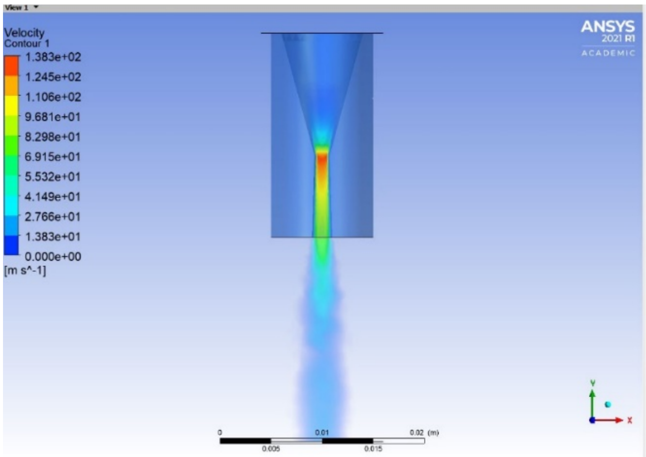

Figure 17. Fourth Nozzle Fluid Velocity Distribution (K-epsilon Model).

When the k-epsilon model was chosen as the turbulence model in flow analysis with the fifth nozzle geometry, it was determined that the velocity of fluid reached a velocity of 84.49 m/s at the nozzle outlet (Figure 18).

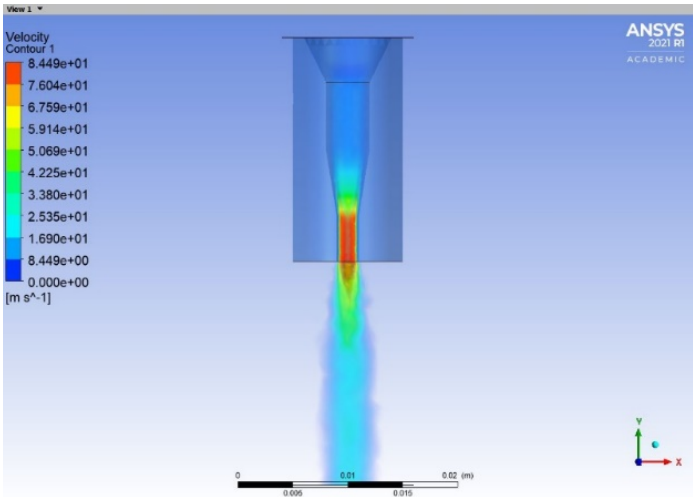

Figure 18. Fifth nozzle fluid velocity distribution (K-epsilon Model).

4. Conclusion

According to the results of the research, it has been determined that even if the nozzle inlet and outlet designs of different nozzle geometries are the same, the change in the internal geometry significantly affects the outlet velocity of the fluid. As a result of the analysis, it was determined that the fastest fluid transfer was at the fourth nozzle; It was determined that the fluid transfer at the lowest velocity was at the fifth nozzle. In the analyzes made with different

Received 25 May 2023; Received in revised form 10 June 2023; Accepted 20 June 2023;
Available online 30 June 2023;
doi: 10.5281/zenodo.8130808

turbulence models, it has been determined that turbulence models do not have a very high effect on the flow velocity of the fluid. However, it has been determined that the use of different turbulence models in the same nozzle geometry affects the flow spray area and amount to a certain extent. In order for the nozzles to be used in different sectors to be designed appropriately, it is of great importance to make the right turbulence model choice by analyzing it with the finite element method.

References

1. Spray Engineering Handbook, CTG SH O7 EU, www.pnr-nozzles.com., PNR Italia srl Via Nenni/Gandini 27058 Voghera (PV) Italia, www.pnr.eu. Accesed: Aug. 5, 20222. [Online]. Available: www.pnrnordic.com/pdf/technical-manual.pdf

2. Onen, B., Fidan, S., Sinmazcelik, T., Cinar, A. (2017). Blasting nozzle Internal geometry effects on wear and roughness of target material in particle erosion. Journal of the Faculty of Engineering and Architecture of Gazi University 32:4 (2017) 1051-1061.

3. Meyer, M., Lupoi, R. (2015). An analysis of the particulate flow in cold spray nozzles. Mechanical Sciences, 6(2), 127.

4. Yin, S., Wang, X. F., & Li, W. Y. (2011). Computational analysis of the effect of nozzle cross-section shape on gas flow and particle acceleration in cold spraying. Surface and Coatings Technology, 205(8-9), 2970-2977.

5. Zeng, L., Bieler, T.R. (2007). Optimal design of a cold spray nozzle by numerical analysis of particle velocity and experimental validation with 316l stainless steel powder, Materials and Design, 28: 2129–2137.

6. Onen, B., Altuncu, E., Cinar, A., (2021). Investigation of the Effects of Different Nozzle Geometries at Erosive Wear Tests on the Wear Track Area and Surface Roughness of PMMA. AKU J. Sci. Eng. 21 (2021) 037101 (755-763) DOI: 10.35414/akufemubid.83736

7. Aksu, T. (2018). The Effects Of Turbulence And Combustion Models On Supersonic Combustion Using Computational Fluid Dynamics. Master Thesis, Tobb University of Economics and Technology Graduate School of Engineering and Science, 152s.

8. Varan, M., , Oylek, I., Dereli, S. (2017). Transient State Finite Element Analysis for Variable Load States of a Three-Phase Synchronous Machine . Gaziosmanpasa Journal of Scientific Research, Cilt/Volume: 6 Sayı/Number: Özel (ISMSIT2017) Yıl/Year: 2017 Sayı/Pages: 59-72

9. F. Moukalled, L. Mangani and M. Darwish, The Finite Volume Method in Computational Fluid Dynamics An Advanced Introduction with OpenFOAM® and Matlab®, Vol. 113, Springer, Switzerland, 4, 2016

10. Ozdemir, Y.H. (2007). Investigation of the flow surrounding the ship by using computational fluid dynamics. Master Thesis, Yıldız Technical University, Institute of Science, 51s, İstanbul.

11. Duz, H. (2013). To Examine Numerically And Experimentally The Laminar-Turbulance Transition Propertıes In Entrance And Fully Developed Flow Region. Doctoral Thesis, Fırat Univ. Institute of Science. Elazığ.

Received 25 May 2023; Received in revised form 10 June 2023; Accepted 20 June 2023;
Available online 30 June 2023;
doi: 10.5281/zenodo.8130808

12. Sukindar, N. A., Ariffin, M. K. A., Baharudin, B. T. H. T., Jaafar, C. N. A., Ismail, M. I. S. (2017). Analysis on temperature setting for extruding polylactic acid using open-source 3d printer. ASPN Journal of Engineering and Applied Sciences, Vol. 12, No. 4, pp. 1348-1353

13. Wilcox, D. C. (1998). Turbulence Modeling for CFD, DCW Industries, Inc. La Canada, California.

14. Shipway P. H., Hutchings, I. M. (1993). Influence of nozzle roughness on condition in a gas-blast erosion rig. wear, 1993, 162–164, 148–158.

15. Onen, B. (2016). Investigating various nozzle geometries for solid particle erosion on polymethyl methacrylate (PMMA). Doctoral Thesis, Kocaeli Univ. Institute of Science. 154s.

Received 25 May 2023; Received in revised form 10 June 2023; Accepted 20 June 2023;
Available online 30 June 2023;
doi: 10.5281/zenodo.8130808